

Phenomenology of low-energy scattering in the framework of quantum chromodynamics

Jorge Dias de Deus and José Emílio Ribeiro

Centro de Física da Matéria Condensada, Instituto Nacional de Investigação Científica, Av. Prof. Gama Pinto 2, 1699 Lisboa-Codex, Portugal

(Received 1 June 1979)

The short-range low-energy interaction between hadrons is studied with the quantum-chromodynamic one-gluon-exchange potential in the context of the resonating-group method. A soft-core approximation is used to estimate low-energy *s*-wave scattering lengths and amplitudes in exotic reactions: K^+p , K^+n , $\pi^+\pi$, and $K^+\pi^+$. Good agreement is found with data.

Recently, one of us¹ applied the techniques of the resonating-group method² (RGM) to nucleon-nucleon low-energy scattering. The nucleons were treated as clusters of three quarks, each cluster belonging to the $(56, L^P=0^+)$ multiplet in the flavor space and to an SU(3) singlet in color. The scattering process was assumed to occur via the formation of a fully antisymmetrized six-quark cluster. The potential used between the quarks was the standard one-gluon-exchange potential of quantum chromodynamics (QCD).^{3,4} The result was quite satisfactory. A repulsive core with the right characteristics for the *N-N* system was found.

In this note, guided by the success of the detailed calculation of Ref. 1, we present a simple method to evaluate scattering lengths and amplitudes in low-energy scattering for hadron collisions.

We start by writing down the radial Schrödinger equation for two particles,

$$\frac{d^2\chi(r)}{dr^2} + [k^2 - U(r)]\chi(r) = 0, \quad (1)$$

with

$$U(r) = \frac{2\mu}{\hbar^2} V(r), \quad (2)$$

where μ is the reduced mass, and $V(r)$ is the potential. Our potential is meant to be a simple equivalent local version of the nonlocal RGM potential. For a collision of two particles *a* and *b*, we write the potential in the form

$$V_{ab}(r) = A_{ab} C_{ab} F(r, R_{ab}). \quad (3)$$

The constant A_{ab} plays, as it were, the role of the square of the quark-gluon effective coupling constant, C_{ab} is like an effective Clebsch-Gordan coefficient, and $F(r, R_{ab})$ is a geometrical factor, controlled by the parameter R_{ab} , measuring the size of the region occupied by the full cluster of quarks. We discuss now the various factors in Eq. (3), starting with the coefficient C_{ab} . The color and color-spin QCD potential between quark *i* (from cluster *a*) and quark *j* (from cluster *b*) can

be written, after averaging in space, in the form

$$\langle V_{ij} \rangle_{\text{space}} = B_{ab} \lambda_i \lambda_j - A_{ab} \frac{m^2}{m_i m_j} \lambda_i \lambda_j S_i S_j, \quad (4)$$

where the λ 's are the SU(3) generators, the S 's are the spin operators, $m_{i,j}$ is the quark mass, and $m^2/m_i m_j = 1$ for quarks of types *u* and *d*.

It is a basic tenet of RGM calculations that the important quantity to evaluate is

$$\left\langle A \sum_{ij} V_{ij} \right\rangle_{\text{SU}(3) \times \text{SU}(2) \times \text{space}}$$

where *A* is the antisymmetrizer and is given by

$$A = \sum_P (-1)^P = 1 - \sum_{\alpha\beta} P^{\alpha\beta}. \quad (5)$$

$P^{\alpha\beta}$ is the interchange operator and interchanges quark (antiquark) α belonging to cluster *a* with quark (antiquark) β of cluster *b*. See Fig. 1(a). Now one has

$$\langle \text{singlet} | \lambda_i \lambda_j | \text{singlet} \rangle_{\text{SU}(3)} = 0. \quad (6)$$

So one sees that one can drop the identity term in (5). Hence, and for all purposes, one can consider *A* to be given by $-\sum_{\alpha\beta} P^{\alpha\beta}$. In other words, we have ensured that the hadron interaction with a quark-quark potential of the type $\lambda_i \lambda_j$ is necessarily short-ranged. One of the QCD potential contributions will be, in general, of the form

$$\sum_{\alpha\beta} \left\langle B_{ab} P^{\alpha\beta} \sum_{i>j} \lambda_i \lambda_j f(r_{ij}) \right\rangle_{\text{SU}(3) \times \text{SU}(6) \times \text{space}}$$

However, in the limit of V_{ij} having no explicit *ij* dependence as in Eq. (4)—only space-averaged quantities matter—the above pure color contribution to $C_{\alpha\beta}$ vanishes because

$$\left\langle P^{\alpha\beta} \sum_{i>j} \lambda_i \lambda_j \right\rangle_{\text{SU}(3)} = 0.$$

Detailed calculation following Ref. 1 shows that this contribution is indeed small even when one retains the explicit spatial dependence in the color

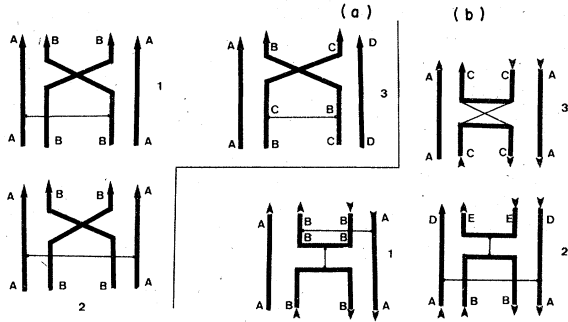


FIG. 1. Relevant quark-exchange diagrams (a) and, as an example, the corresponding annihilation ones (b) [obtained from (a) by crossing $s-u$].

potential. (The smallness of $\langle P^{ab} \rangle_{\text{SU}(6)}$, provides an alternative argument for neglecting the term in $\lambda_i \lambda_j$.)

We are then left with the color-spin term as the sole contribution to C_{ab} :

$$C_{ab} = \sum_{\alpha\beta} \left\langle \sum_{i>j} P^{\alpha\beta} \frac{m^2}{m_i m_j} \lambda_i \lambda_j S_i S_j \right\rangle_{\text{SU}(3) \times \text{SU}(6)}. \quad (7)$$

The values of C_{ab} , calculated for several interesting hadron-hadron elastic processes, are given in Table I.

We discuss next $F(r, R_{ab})$. This factor is clearly related to the overlap for the two hadron wave functions. We simply approximate it by

$$F(r, R_{ab}) = \begin{cases} 1, & r < R_{ab} \\ 0, & r > R_{ab} \end{cases}. \quad (8)$$

Depending on the sign of C_{ab} [Eq. (7)], our hadron-hadron potential will then be either a soft-core repulsive potential ($C_{ab} > 0$) or an attractive square well ($C_{ab} < 0$). From the positive values of C_{ab} in Table I and the nature of the V_{ij} potential [Eq. (4)], we see that we are dealing with a short-range re-

pulsive potential.

We try now to justify the assumption (8), in the context of the resonating-group method and Ref. 1. It was a feature of the $N-N$ relative s -wave function obtained in Ref. 1 to have a physical node at around 0.36 fm. This node was found to be almost insensitive to the c.m. energies up to 100 MeV, starting then to move slowly inwards with the energy (see Fig. 2). The wave function, extending from 0 to about 1 fm, hardly changes within a large energy range. In the limit of small relative momentum k , we see from Fig. 2 that we can approximate $\psi_{N-N}(r)$ by

$$\psi_{N-N}(R) = \sinh[K(r - 0.36 \text{ fm})], \quad (9)$$

with

$$K = (U_{NN} - k^2)^{1/2} \quad (10)$$

and $U_{NN} = 12 \text{ fm}^{-2}$. Now one clearly sees that

$$\sinh[K(r - 0.36)]_{r \approx 1 \text{ fm}} \approx \sinh[Kr]_{r \approx 1 \text{ fm}},$$

and this is what justifies the use, in the low-energy region, of a soft core of height U_{NN} and range $R \sim 1 \text{ fm}$: $\sinh[Kr]$ is precisely the inner solution of such a potential. The s -wave δ_0 phase shift, computed with our soft-core potential ($U_{NN} = 12 \text{ fm}^{-2}$, $R_{NN} = 1 \text{ fm}$), agrees with theoretical results of Ref. 1, and the agreement is good even beyond the strictly very-low-energy domain.

Finally, the factor A_{ab} in the hadron-hadron potential (3) represents the QCD coupling parameter α_s integrated over the hadron wave function.

Our potential is now fully specified. For each ab process, two parameters have to be given: A_{ab} (the effective coupling constant) and R_{ab} (the effective size of the region occupied by the two hadron cluster). However, they can be estimated from different physical arguments, and thus their magnitude is not free. In the NN case,¹ A_{NN} was determined from the $N-\Delta$ mass difference A_{NN}

TABLE I. s -wave scattering lengths (prediction and experimental results) for $(kN)_{I=1, I=0}$, $(\pi\pi)_{I=2}$, $(k\pi)_{I=3/2}$. The values of A_{ab} and R_{ab} are assumed universal and taken from the theoretical discussion of NN scattering in Ref. 1. When required, we used $m_s/m_{u,d} = \frac{5}{3}$.

Process $a \ b$	A_{ab} (fm^{-1})	R_{ab} (fm)	C_{ab}	Prediction (fm)	Exper. (fm)
$(KN)_{I=1}$	0.37	1	$(2 + \frac{1}{2} \frac{m}{m_s}) \frac{1}{9}$	-0.39	~ -0.3 (Ref. 5)
$(KN)_{I=0}$	0.37	1	$(2 + \frac{1}{2} \frac{m}{m_s}) \frac{5}{9}$	-0.31	~ -0.23 (Ref. 6)
$(\pi\pi)_{I=2}$	0.37	1	$\frac{8}{9}$	-0.072	~ -0.042 (Ref. 7)
$(K\pi)_{I=3/2}$	0.37	1	$(\frac{1}{2} + \frac{1}{2} \frac{m}{m_s}) \frac{8}{9}$	-0.087	

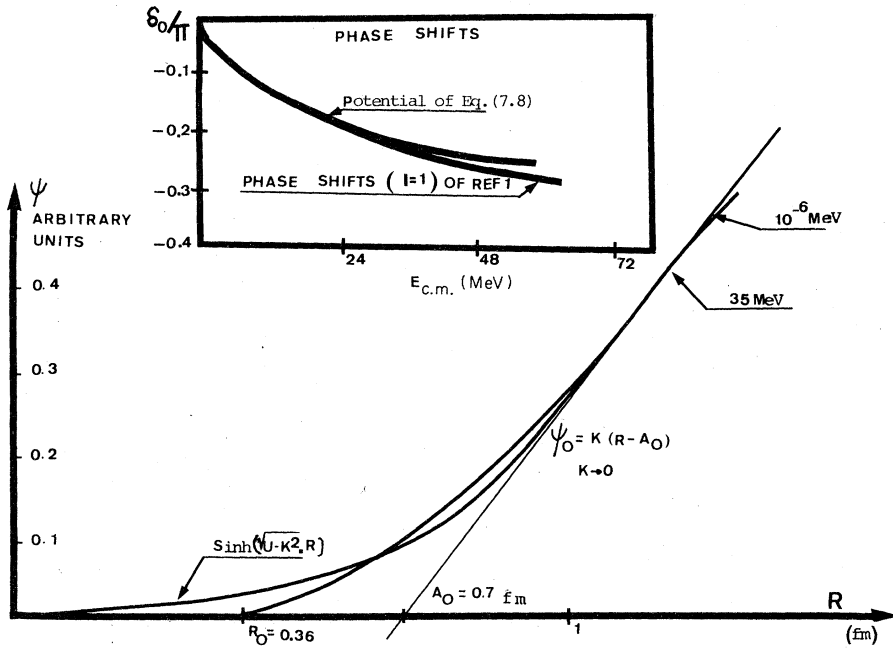


FIG. 2. *Figure below:* $(N-N)_{I=1}$ relative s -wave functions (full RGM calculation). Also depicted is the $\kappa \rightarrow 0$ asymptotic limit of the wave function showing a scattering length of ≈ 0.7 fm as obtained by $\lim_{\kappa \rightarrow 0} [\delta_0(\kappa)/\kappa]$. *Figure above:* Comparison of the soft-core produced s -wave phase shifts with the RGM ones. Both are for the $(NN)_{I=1, s=0}$ scattering.

$\approx 0.37 \text{ fm}^{-1}$, and R_{NN} should be of the order of twice the radius parameter R_0 in the nucleon wave function $R_{NN} \sim 2R_0 \sim 1 \text{ fm}$ (see also Fig. 2). With $A_{NN} = 0.37 \text{ fm}^{-1}$ ($U = 12 \text{ fm}^{-2}$) and $R_{NN} = 1$, we fitted, as mentioned above, the repulsive NN phase shifts of Ref. 1. For the other reactions, we assume universality of A_{ab} and R_{ab} ,

$$R_{ab} = R_{NN} = R, \quad (11)$$

and, as a consequence,

$$A_{ab} = A_{NN} = A. \quad (12)$$

Equation (11) means that all (light-quark) hadrons have roughly the same size, as follows from elec-

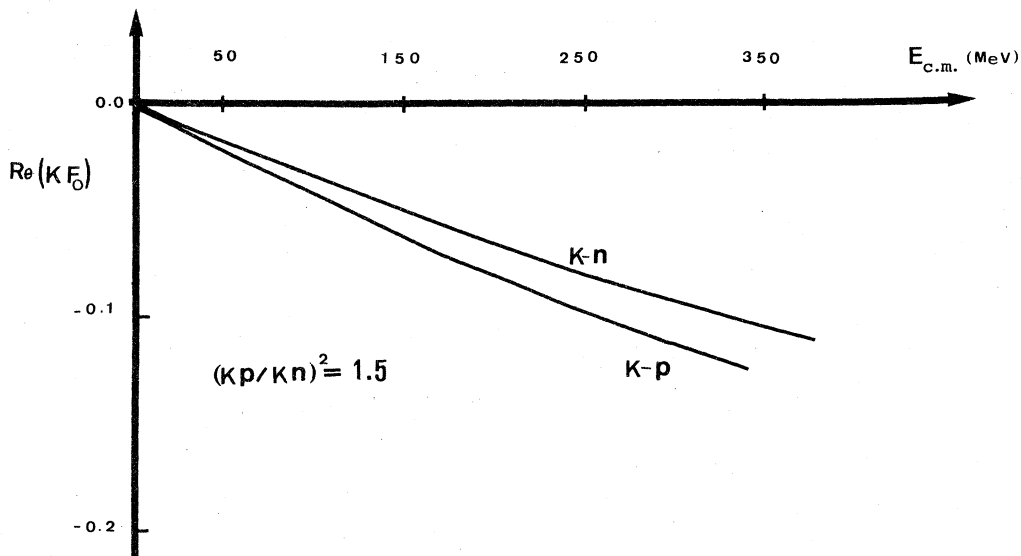


FIG. 3. Plots of the real part of the s -wave amplitude for the K^+p and K^+n scattering as a function of the c.m. momentum.

tromagnetic form factors and diffractive-cross-section slopes.

Before proceeding, one should mention that the diagrams we compute [Fig. 1(a)] are not the only possible one-gluon-exchange diagrams. If flavor annihilation is allowed [see Fig. 1(b)], contributions with gluon exchange in the direct channel should be included. These contributions should, in this scheme, be responsible for attractions. In other words, our calculation with diagrams of Fig. 1(a) should only apply to exotic processes. Regarding the calculations, it is straightforward to evaluate the s -wave phase shifts $\delta_0(k)$ produced by the potential (3) defined above,

$$\cot\delta_0(k) = \frac{K \coth(KR) \cot(kR) + k}{-k \coth(kR) + K \cot(KR)}. \quad (13)$$

with the scattering length a_0 given by

$$a_0 = -\frac{(\sqrt{UR}) \coth(\sqrt{UR}) - 1}{(\sqrt{UR}) \coth(\sqrt{UR})} R. \quad (14)$$

In Table I, we present our results in comparison with experiment. We did not try to adjust the parameters. The scattering lengths tend to be overestimated in absolute value, and this may be due to the fact that the parameter R_{ab} should be smaller for pions and kaons than for nucleons. In Fig. 3 we show plots of the real part of the s -wave amplitudes

$$\text{Re}(kf_0) = \frac{\sin 2\delta}{2}$$

in K^*N scattering as a function of the c.m. momentum. The curves are in the approximate constant ratio 1.5, close to what is experimentally observed.⁸

For the elastic processes ϕp and ψp which are exotic, the diagrams of Fig. 1 give no contribution, because no quarks can be exchanged. So elastic scattering, compared to inelastic scattering, is very small even at low energies. The rapid rise of the cross section with the opening of inelas-

tic channels is a well known effect in ψp scattering. In πN scattering, both diagrams, Figs. 1(a) and 1(b), contribute. If the quark annihilation is flavor independent (presumably, a reasonable approximation for u, d quarks), one obtains a larger net repulsion in $\pi^* p$ than in $\pi^- p$, as is in fact observed. Finally, repulsion is totally absent in annihilation channels ($h\bar{h}$), and attractive diagrams of Fig. 1(b) should then dominate completely.⁹

The color-spin potential we used here is the one responsible for mass differences in hadrons.³ The reason we obtain s -wave repulsion stems from the same fact that forbids resonances in the exotic channels: The color-spin interaction is not strong enough to produce attraction and, therefore, produce composite hadrons which are relatively stable against decaying.⁴ The physical connection between the absence of such states and the presence of repulsion is very transparent here, and it gives support to the QCD color-spin calculation in low-energy hadron-hadron processes. On the other hand, it is very tempting to interpret the diagrams of Figs. 1(a) and 1(b) as the first contributions (lowest order, short range) in building up the multi-gluon planar diagrams of the dual model $V(u, t)$ and $V(s, t)$ diagrams, respectively.

We have only considered leading α_s diagrams. The belief is that, because of the asymptotic free character of the theory, one-massless-gluon exchange dominates at short distances and low partial waves. As the distance increases, multigluon exchanges become increasingly important and dominate high partial waves. Such expectation is exactly the opposite of what happens in the description of the potential in terms of massive meson exchanges: Single-meson (pion) exchange dominates high partial waves and multimeson exchanges dominate s waves. While, for large distances, the conventional description is perhaps simpler, for low partial waves a microscopic quark description may be more adequate.

¹J. E. Ribeiro, D. Phil. Thesis Oxford, 1978 (unpublished); see also D. A. Liberman, Phys. Rev. D **16**, 1542 (1977).

²J. Wheeler, Phys. Rev. **52**, 1083 (1937); **52**, 1107 (1937).

³A. De Rújula, H. Georgi, and S. Glashow, Phys. Rev. D **12**, 147 (1975).

⁴K. Johnson, in *Fundamentals of Quark Models*, proceedings of the Seventeenth Scottish Universities Summer School in Physics, St. Andrews, 1976, edited by I. M. Barbour and A. T. Davis (SUSSP Publications,

Edinburgh Univ., Edinburgh, 1977).

⁵U. Pilkuhn *et al.*, Nucl. Phys. **B65**, 460 (1973).

⁶B. R. Martin, J. Phys. G **4**, 335 (1978).

⁷J. L. Petersen, CERN Report No. CERN 77-04, 1977 (unpublished).

⁸See, for instance, Carl Dover, BNL report (unpublished).

⁹M. Chaichain, R. Kogerler, and M. Roos, Nucl. Phys. **B141**, 110 (1978).